Materials Science Forum *Online: 2010-01-12*
ISSN: 1662-9752, Vols. 638-642, pp 1288-1293
doi:10.4028/www.scientific.net/MSF.638-642.1288

Recrystallization textures in heavily cold-rolled Ni_3Al based single crystals

Masahiko Demura[1, a], Ya Xu[1,b] and Toshiyuki Hirano[1,c]

[1]National Institute for Materials Science, 1-2-1 Sengen, Tsukuba, Ibaraki 305-0047, Japan

[a]DEMURA.Masahiko@nims.go.jp, [b]XU.Ya@nims.go.jp, [c]HIRANO.Toshiyuki@nims.go.jp

Keywords: Intermetallics, Two-phase alloys, Ni-base superalloys, Electron backscattered diffraction method

Abstract. Texture evolution during recrystallization and grain growth was examined for a Ni_3Al/Ni two-phase single crystal (binary Ni-18 at.% Al) 83% cold-rolled, then compared with that for a Ni_3Al single-phase single crystal (Ni-24 at.% Al). The cold-rolled single crystal had a sharp {110}<001> (Goss) texture. When it was recrystallized at 873K, the texture changed into a complicated one consisting of several components. Most of them had a special rotation relationship to the original Goss texture, i.e. 40˚ about <111>, which special relationship was similarly observed in the single-phase case. The 40˚<111> texture became shaper with no quantitative change as the grain growth proceeded. This high stability of the recrystallized texture contrasted with the single-phase case in which the authors previously found that the texture returned to the original Goss texture. The difference was discussed based on the orientation analysis by an electron backscattered diffraction method.

Introduction

Heat-resistant metallic foils and sheets are one of the key materials in high-temperature micro-scale systems, e.g. a chemical reactor to produce hydrogen. One of the promising materials is an intermetallic compound Ni_3Al and its based alloy consisting of Ni_3Al and Ni solid-solution phases (Ni_3Al/Ni two-phase alloys, or so-called Ni-base superalloys), since they have excellent mechanical properties and corrosion/oxidation resistance at high temperatures [1]. We've recently developed their foils by cold rolling [2-6], which became possible using single crystalline ingots as a starting material [7]. Furthermore, we've found that they exhibit a catalytic activity for hydrogen production reactions such as methanol decomposition [8-12] and methane steam reforming [13,14]. Thus, the Ni_3Al based foils can be used as a container and a catalyst in the micro chemical reactor for hydrogen production consequently.

When they are in service at elevated temperatures, recrystallization and grain growth occur in such heavily cold-rolled metallic foils. In the single-phase Ni_3Al, we've found a very interesting phenomenon on the texture evolution during the recrystallization and grain growth, as follows

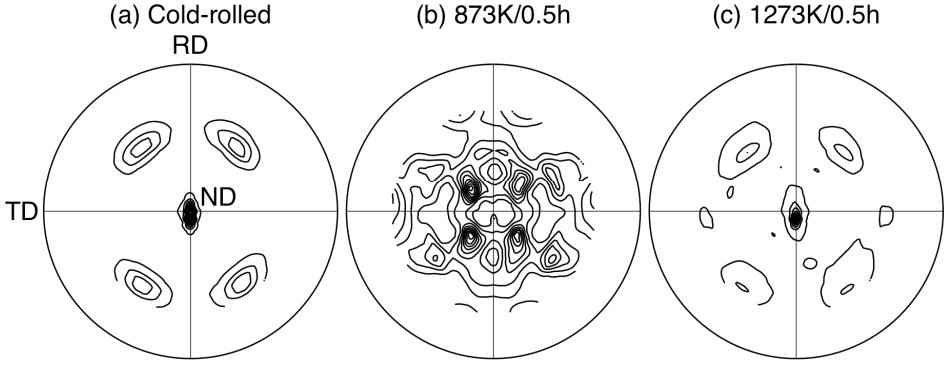

Fig. 1 {220} pole figures for the Ni_3Al single-phase single crystal: (a) 84% cold-rolled, (b) subsequently heat-treated at 873K/0.5h after the cold rolling, and (c) at 1273K/0.5h.

[15-17]. First, the cold-rolled foil had a strong {110} texture, as shown in Fig. 1(a). The recrystallization was completed at 873K and the texture changed into a complicated one consisting of several components different from the original {110} texture (Fig. 1(b)). Most of the components were revealed to have a specific rotation relationship to the cold-rolled texture: 40˚ about <111> axis. Surprisingly, the texture returned to the same {110} texture as the cold rolled one after the grain growth at higher temperatures, typically 1273K (Fig. 1(c)). We describe this phenomenon as *texture memory effect*.

We here examined the textures in the Ni_3Al/Ni two-phase single crystal 83% cold-rolled and subsequently heat-treated, paying attention to whether or not the texture memory effect occurred. The results were compared with those in the single-phase Ni_3Al.

Experimental procedures

A single-crystalline sheet of binary Ni-18 at.% Al having a Goss orientation, grown by an investment cast method, was 83% cold-rolled to the thickness of 315 μm without any intermediate annealing steps; the fabrication process was the same as reported in our previous papers [4,6]. Specimens cut from the cold-rolled foil by electric discharging machining were subsequently heat-treated at 873k or 1273k for 0.5h or 100h in a flowing Ar gas atmosphere after evacuation down to 10^{-3} Pa in advance. The {220} pole figure was measured on the specimen surface, lightly polished, by the X-ray Schultz back reflection method. The microstructure was observed from the longitudinal section of the foil specimens by using a scanning electron microscope with a field emission gun (SEM, JEOL JSM-7000F). The orientations of the recrystallized grains were measured on the specimen surface by the electron backscattered diffraction methods (EBSD, TSL OIM4) in the same SEM: the thickness of ~100 μm was mechanically polished to eliminate a surface effect. Since the crystal structure of Ni_3Al, i.e. $L1_2$, is based on an fcc structure, it was hard to distinguish between the Ni_3Al phase and the Ni, fcc phase in the present EBSD analysis, and both the phases were thus recognized as an fcc phase.

Results and discussion

Texture evolution. Fig. 2 shows the {220} pole figures for the cold-rolled specimen and the subsequently heat-treated ones of the Ni_3Al/Ni two-phase single crystal. The cold-rolled specimen retains a Goss texture (Fig. 2(a)). The stability of the Goss orientation in the cold rolling deformation was similarly observed in the single-phase Ni_3Al [16]. Our previous study showed that the two-phase single crystals with the same composition as the present alloy exhibited very similar texture evolution to that in the Ni_3Al single-phase single crystals [6].

The Goss texture changes into a complicated one consisting of several orientation components after heat treatment at 873K/0.5h (Fig. 2(b)), by which heat treatment recrystallization was almost

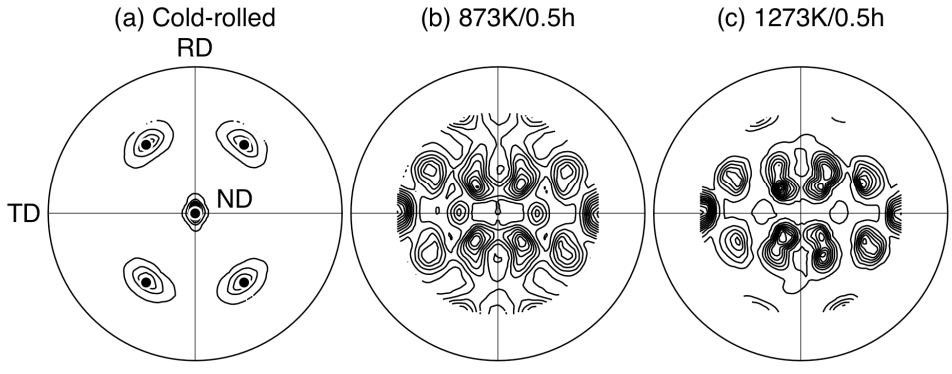

Fig. 2 {220} pole figures for the Ni_3Al/Ni two-phase single crystal: (a) 84% cold-rolled, (b) subsequently heat-treated at 873K/0.5h after the cold rolling, and (c) at 1273K/0.5h. The 110 poles of the Goss orientation are shown by the dots in (a).

completed according to the EBSD analysis. Each component is different from the Goss orientation, suggesting that the recrystallized grains have new orientations. The shape of the contour map seems similar to that for the single-phase Ni_3Al (compare with Fig. 1(b)), in which case the recrystallized texture had a 40˚ rotation relationship about <111> axis to the original Goss orientation. In fact, the same rotation relationship is found in most of the recrystallized grains in the present alloy by the EBSD analysis as will be described later.

The recrystallized texture, i.e. the 40˚<111> rotated Goss texture, becomes shaper in the specimen heat-treated at 1273K/0.5h, keeping a similar shape, as shown in Fig. 2(c). A much longer heat treatment up to 100h at this temperature did not bring a qualitative change in the texture. Thus, the texture formed during the recrystallization was stable even at such high temperature and showed no sign of further changing into another one by grain growth. This high stability of the recrystallized texture contrasts with the single-phase case, where the Goss texture was again developed after the heat treatment at 1273K/0.5h. These results clearly show that the return to the cold-rolled texture, or the texture memory effect, did not occur in the two-phase single crystal.

Two-phase microstructures. Fig. 3 shows backscatter electron images (BEIs) obtained form the longitudinal section, i.e. the normal direction (ND) – transversal direction (TD) section. In the cold-rolled state (Fig. 3(a)), the Ni_3Al particles (the darker contrast) are elongated along the rolling direction (RD) and compressed along the ND. The thickness of them ranges from 0.1 to 0.4 μm. Such elongated pancake-type shape shows that the Ni_3Al particles, harder than the Ni matrix, are plastically deformed by cold rolling; and naturally, the Ni matrix is also deformed. Our previous TEM observation revealed that a large number of dislocations were accumulated on slip planes in the Ni_3Al elongated pancakes, while they were rearranged into a cell structure in the Ni matrix [6].

The elongated pancake shape must be unstable and a spherical or cubic shape has a lower free energy in Ni_3Al/Ni two-phase alloys [18]. Hence, it will start to change when the Ni and Al atoms can diffuse at a high temperature. The specimen heat-treated at 873K/0.5h still retained the elongated pancake structure as shown by Fig. 3 (b). This is likely because an interdiffusion distance of Ni and Al atoms was too short at this condition to change the outer shape. Despite such unchanged of the elongated pancake structure, the recrystallization had occurred, accompanied with the visible changed in the texture, as mentioned in the earlier subsection (Fig. 2(b)). The grain size was 0.4 μm in average, measured by the EBSD analysis. Noted that the size is virtually equivalent to the thickness of the elongated pancakes, suggesting that they acted as obstacles for the grain growth in this two-phase system.

The shape of the Ni_3Al particles finally changed at 1273K for 0.5h. Fig. 3 (c) shows that they have a blocky shape covered by flat interfaces. The comparison between the BEI and the EBSD orientation map revealed that most of the Ni_3Al particles existed coherently in the Ni matrix. The flatness of the interfaces suggests that they are parallel to {100}, keeping so-called cube-on-cube, low-energy configuration [18], though they are not perfect cubic. The size of them ranges from 1 to 2 μm, and is

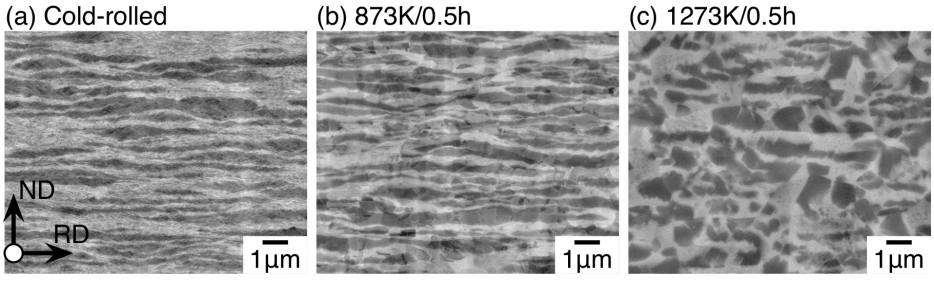

Fig. 3 Backscatter electron images for longitudinal microstructures of the Ni_3Al/Ni two-phase single crystal: (a) 84% cold-rolled, (b) subsequently heat-treated at 873K/0.5h after the cold rolling, and (c) at 1273K/0.5h. The darker and brighter contrasts correspond to the Ni_3Al and Ni solid solution phases, respectively.

close to the grain size, which was 1.5 μm in average. This equivalence again supports the idea that the grain growth would be hindered by the existence of the Ni_3Al particles.

Recrystallization microstructure by EBSD analysis. It turned out that the texture evolution with the progress of grain growth was different from that in the single-phase Ni_3Al, despite the similarity in the recrystallization texture (compare Fig. 1 and 2). This suggest that there may be a little difference in the microstructure and/or the minor texture component just after the recrystallization, which difference would become larger as the grain growth proceeds. We thus measured the orientation map just after the recrystallization, i.e. in the specimen heat-treated at 873K/0.5h, using the EBSD method; and the results are shown in Fig. 4. Most of the recrystallized grains have 40˚<111> rotated Goss orientations (colored as light grey) as shown in Fig. 4(a). In detail, there are a small number of regions having a Goss orientation (dark grey), which Goss component was not detected by the X-ray texture measurement. These Goss regions are very small, compared with the other, recrystallized grains. It is hard to judge whether they are recrystallized grains or no recrystallization occurs locally there. They can be assumed to disappear when grain growth proceeds, because their size is smaller than the other grains. In fact, the Goss regions were rarely observed after the grain growth at 1273K/0.5h even by the EBSD analysis; instead, almost all the grains were 40˚<111> rotated Goss. These results, i.e. the diminishment of the minor Goss regions and the sharpening of the 40˚<111> rotated Goss texture are consistent with the texture evolution measured by the X-ray method.

Similarly, in the single-phase Ni_3Al, the 40˚<111> rotated Goss grains were in the majority and the Goss grains were in the minority [16]. However, the size of the Goss grains was different: it was *relatively* large, compared with those of the other grains (see Fig. 4(b)). Furthermore, they grew faster than the other, resulting in the return to the Goss texture by grain growth.

Texture formation mechanism. The EBSD analysis revealed the similarity in the formation of the 40˚<111> rotated grains and the difference in the relative size of the minor Goss grains or regions. First, we consider that the formation mechanism of the 40˚<111> rotated Goss grains is the same between the single-phase and the two-phase alloys. In the single-phase Ni_3Al, it was explained assuming that a boundary between two grains having a 40˚<111> rotated relationship has a high mobility, compared with the other, general boundaries [16]. That is, the 40˚<111> rotated Goss grains grew faster since they were surrounded by the high-mobility boundary in the Goss texture. The assumption of the high mobility of this special boundary is widely valid in fcc metals and alloys [19].

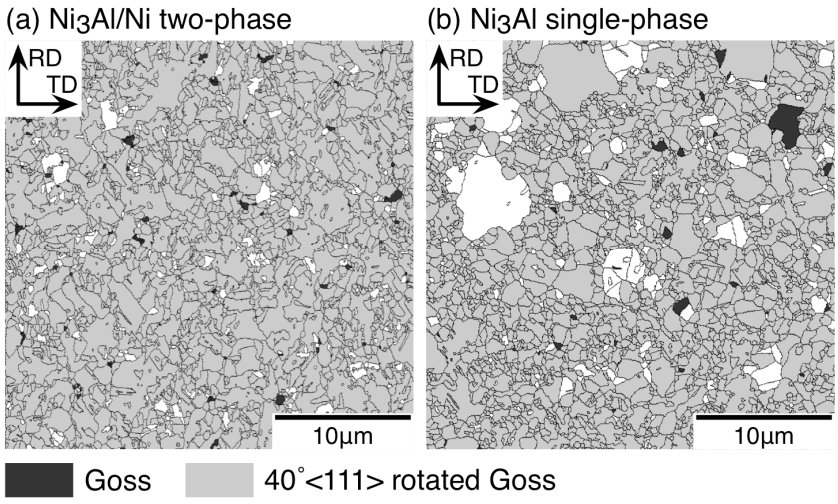

Fig. 4 Orientation maps obtained on the RD-TD section of the cold-rolled and subsequently heat-treated at 873K/0.5h, which condition corresponds to the early stage of grain growth just after the recrystallization, by the EBSD analysis: (a) the Ni_3Al/Ni two-phase and (b) the Ni_3Al single-phase.

The same mobility-based explanation can thus apply to the present two-phase alloy consisting of the fcc and the fcc-based phases.

In the recrystallization process, other types of grains are also nucleated. Among them, a grain having the Goss orientation can grow faster from the same assumption when it encounters one of the 40˚<111> rotated Goss grains. The possibility for this encounter increases as the number of the 40˚<111> rotated Goss grains increases with the progress of the recrystallization. That is, after the recrystallization, where the 40˚<111> rotated Goss grains become dominant, the Goss grains can grow faster. Thus, the mobility-based mechanism can also explain the return to the original Goss texture observed in the single-phase case.

However, it did not work for the Goss grains or regions in the two-phase alloy. This means that the nucleation or the growth of them was hindered in the two-phase microstructure. As we mentioned earlier, the two-phase structure seems to limit the movement of the grain growth. Doherty pointed out that the coherent particles such as the Ni_3Al in the present two-phase system would be effective in restraining grain-boundary motion [20]. Probably because of this restraining effect, the Goss grains were not able to grow over the size of the two-phase structure, i.e. the thickness of the elongated pancake-shape Ni_3Al particles, even though they were surrounded by the high-mobility grain boundary. This may cause the diminishment of the Goss grains during the grain growth. In other words, the mobility-based mechanism worked until the grain size reached to the limitation by the two-phase microstructure, in which stage the 40˚<111> rotated Goss grains became dominant. Then, once the grain growth was hindered by the Ni_3Al particles, this mechanism did not work and thus no texture return occurred.

Conclusions

The texture evolution during the recrystallization and grain growth was examined in the Ni_3Al/Ni two-phase single crystal with the Goss texture and the following results were obtained:

1. The recrystallization texture mainly consisted of the 40˚<111> rotated Goss components, similarly to the Ni_3Al single-phase single crystal.
2. It became shaper with the grain growth, showing no qualitative change. Thus, the texture memory effect, which occurred in the single-phase case, did not occur.
3. The EBSD analysis revealed that there were a few Goss grains in the recrystallized microstructure. They were very small and disappeared with the grain growth. The limitation in the growth of the Goss grains, probably due to the two-phase microstructure, was found to yield the sharpening of the recrystallization texture instead of the texture return. On the contrary, in the single-phase Ni_3Al, the minor Goss grains were relatively large just after the recrystallization and then grew faster than the other, resulting in the return to the original Goss texture with the progress of the grain growth.

Acknowledgements

The authors thank M. Takanashi for his helpful assistance in the sample preparation.

References

[1] N.S. Stoloff: Int. Mater. Rev. Vol. 34 (1989), p. 153.

[2] M. Demura, Y. Suga, O. Umezawa, K. Kishida, E.P. George and T. Hirano: Intermetallics Vol. 9 (2001), p. 157.

[3] M. Demura, K. Kishida, Y. Suga and T. Hirano: Metall. Mater. Trans. A Vol. 33A (2002), p. 2607.

[4] M. Demura, K. Kishida, Y. Suga, M. Takanashi and T. Hirano: Scripta Mater. Vol. 47 (2002), p. 267.

[5] H. Borodians'ka, M. Demura, K. Kishida and T. Hirano: Intermetallics Vol. 10 (2002), p. 255.

[6] D. Li, K. Kishida, M. Demura and T. Hirano: Intermetallics Vol. 16 (2008), p. 1317.

[7] K. Kishida, M. Demura, Y. Suga and T. Hirano: Phil. Mag. Vol. 83 (2003), p. 3029.

[8] Y. Xu, S. Kameoka, K. Kishida, M. Demura, A.-P. Tsai and T. Hirano: Mater. Trans. Vol. 45 (2004), p. 3177.

[9] Y. Xu, S. Kameoka, K. Kishida, M. Demura, A.-P. Tsai and T. Hirano: Intermetallics Vol. 13 (2005), p. 151.

[10] Y. Xu, S. Kameoka, K. Kishida, M. Demura, A.-P. Tsai and T. Hirano: Mater. Sci. Forum Vol. 475-479 (2005), p. 755.

[11] D.-H. Chun, Y. Xu, M. Demura, K. Kishida, M.-H. Oh, T. Hirano and D.-M. Wee: Catalysis Letters Vol. 106 (2006), p. 71.

[12] D.-H. Chun, Y. Xu, M. Demura, K. Kishida, D.-M. Wee and T. Hirano: J. Catalysis Vol. 243 (2006), p. 99.

[13] Y. Ma, Y. Xu, M. Demura, D.H. Chun, G. Xie and T. Hirano: Catalysis Letters Vol. 112 (2006), p. 31.

[14] Y. Ma, Y. Xu, M. Demura and T. Hirano: Applied Catalysis B: Environmental Vol. 80 (2008), p. 15.

[15] M. Demura, K. Kishida, Y. Xu and T. Hirano: Mater. Sci. Forum Vol. 467-470 (2004), p. 447.

[16] M. Demura, Y. Xu, K. Kishida and T. Hirano: Acta mater. Vol. 55 (2007), p. 1779.

[17] M. Demura, Y. Xu and T. Hirano: Mater. Sci. Forum Vol. 539-543 (2007), p. 1513.

[18] A. Baldan: J. Mater. Sci. Vol. 37 (2002), p.2379.

[19] G. Gottstein and Shvindlerman: *Grain Boundary Migration in Metals: Thermodynamics, Kinetics, Applications* (CRC Press, USA 1999)

[20] R.D. Doherty: Metal Science Vol. 16 (1982), p. 1.